Image Anal Stereol 2022;41:193-202 doi: 105566/ias.2791
Original Research Paper

ANALYSIS OF UTERINE MORPHOLOGY IN OVARIECTOMIZED RATS TREATED WITH ALENDRONATE AND HOP EXTRACT USING OPEN-SOURCE SOFTWARE

EDI ROĐAK[1], NADA ORŠOLIĆ[2], ROBERT GRGAC[3,4], JASMINA RAJC[5,6], MARINA BAKULA[5], NIKOLA BIJELIĆ✉,[1]

[1]Department for Histology and Embryology, Faculty of Medicine Osijek, University of Osijek, J. Huttlera 4, 31000 Osijek, Croatia; [2]Department of Animal Physiology, Faculty of Science Zagreb, University of Zagreb, Rooseveltov trg 6, Zagreb, Croatia; [3]Institute of Entomology, Biology Centre, Czech Academy of Sciences, Branišovská 1160/31, 37005 České Budějovice, Czechia; [4]Faculty of Science, University of South Bohemia, Branišovská 1645/31a, 37005 České Budějovice, Czechia; [5]Department of Pathology and Forensic Medicine, University Hospital Centre Osijek, J. Huttlera 4, 31000 Osijek, Croatia; [6]Department of Pathology and Forensic Medicine, Faculty of Medicine Osijek, University of Osijek, J. Huttlera 4, 31000 Osijek, Croatia
e-mail: erodak@mefos.hr; nada.orsolic@biol.pmf.hr; robert.grgac@entu.cas.cz; rajcjasmina@gmail.com; bakula.marina@gmail.com; nbijelic@mefos.hr

(Received, August 29, 2022; accepted October 10, 2022)

ABSTRACT

Free and open-source software for image analysis and morphological measurements in scientific research is rising in popularity and capabilities as new methods, plugins and macros are being actively developed. A semi-automated method for measuring rat uterus morphology using free and open-source software (Gimp and FIJI) is demonstrated in this paper. Research was performed on ovariectomized rats as a model of osteoporosis (with sham-operated control group). The animals were treated with alendronate, hop extract or the combination of the two. Whole histological slides were photographed and images were manually pre-processed in Gimp. Color masks from Gimp were loaded in FIJI and polar transformation and measurements were made using a custom macro. This analysis was supplemented by manual assessment of Ki67 proliferation marker expression by a pathologist. Our results suggest that monotherapy or combination therapy with alendronate and hop extract does not cause proliferation of the endometrium in ovariectomized rats and would be safe for use in osteoporosis treatment in this regard. The semi-automated method used in this research is more precise and unbiased than older manual methods. Furthermore, it can be easily adapted for analysis of whole-slide images of almost any round or oval organ.

Keywords: alendronate, hop extract, image analysis, open-source, osteoporosis, uterus.

INTRODUCTION

FREE AND OPEN-SOURCE SOFTWARE IN BIOMEDICAL IMAGE ANALYSIS

Image analysis in biological studies is moving away from semi-quantitative manual analysis and steering in direction of obtaining exact numerical data through the usage of digital technologies for image processing and analysis. Some image processing and analysis software packages are proprietary and are used only with a specific instrument (e.g. a microscope or a CT scanner), while others are open-source and developed by individuals or organizations in the scientific community.

Proprietary software often comes with a significant price tag. This may be out of reach of scientific teams in developing countries, or small laboratories with limited funding. It is not surprising, then, that free and open-source image analysis programs are being increasingly developed, perfected, and used in scientific biomedical image analysis. Probably the best example is ImageJ, created 35 years ago as NIH Image, which became ImageJ and soon stimulated creation of different plugins and even ImageJ-based distributions, such as FIJI. All this work was driven by the needs of researchers rather than by profit and market (Schindelin *et al.*, 2012; Schneider *et al.*, 2012; Rueden *et al.*, 2017).

These programs have become more powerful as computing capabilities of modern computers increased, so nowadays many of these software packages support large, whole-slide images, which contain very large amount of data (Aeffner *et al.*, 2019). Some programs can

be integrated with online platforms for controlled access to images and their metadata, such as OMERO, an open source platform (Burel *et al.*, 2015). Some open access programs also offer the flexibility of writing custom plugins or macros that can be tailored to specific projects which might be out of scope for proprietary software. These and other developments in the field have led to an unprecedented collection and analysis of biomedical images for scientific research in recent decades (Schneider *et al.*, 2012).

Furthermore, some studies require that the images be edited or combined before the measurements are made or simply for a better presentation of the results. Probably the most popular software for that purpose is a proprietary program Adobe Photoshop. There are free and open-source alternatives to this software, such as GIMP (GNU image manipulation program by GIMP Development Team, 2022. Available at: https://www.gimp.org.), which is one of the most used and most functional such programs and is available for Linux, Windows and macOS (Solomon, 2009; Sedgewick, 2017).

OSTEOPOROSIS, PHYTOESTROGENS, AND REPRODUCTIVE ORGANS

Osteoporosis is a metabolic disorder of the skeletal system characterized by the reduction of bone mass and increased bone fragility (Ensrud and Crandall, 2017). Primary osteoporosis is caused by the physiological reduction in sex hormone levels in older age, while secondary osteoporosis is, by definition, osteoporosis with a different and clearly definable etiology, such as adverse reactions to medication and other (Dobbs *et al.*, 1999; Ji and Yu, 2015).

In the second half of the 20th century, estrogen replacement therapy was used for the treatment of osteoporosis, however, research in late 20th and early 21st century showed that estrogen therapy was related to increased risk of breast cancer and cardiovascular diseases. Therefore, bisphosphonates a took major role in treating osteoporosis in modern medicine, and the use of selective estrogen receptor modulators (SERMs) increased in recent decades (Tella and Gallagher, 2014; An, 2016). Bisphosponates are synthetic analogues of pyrophosphate which inhibit bone resorption through several mechanisms, prominent members of the group being alendronate, risendronate and ibandronate (Drake *et al.*, 2008).

Recent research focused on using phytoestrogens from different plants in the treatment of postmenopausal symptoms, such as hot flashes, and the data show that they are effective to a certain extent, without significant side-effects (Chen *et al.*, 2015). Research also showed that phytoestrogens from soybean, hops and other sources can inhibit bone loss and help the in prevention of osteoporosis both in animals and humans and are being considered as candidates for osteoporosis prevention and treatment (Fu *et al.*, 2014; Słupski *et al.*, 2021). One of the recent candidates for research is 8-prenylnaringenin (8PN), the most potent phytoestrogen in hops, and one of the most potent phytoestrogens known to date. Although 8PN content in hops is relatively low, cytochrome P450 in the liver and certain microbes in distal colon can transform prenylated isoflavones from hops (xanthohumol and isoxanthohumol) into 8PN (Guo *et al.*, 2006; Possemiers *et al.*, 2006). 8PN has a high affinity for estrogen receptors (ER), with a preference for ERα over ERβ. ERα expression is prevalent in uterus, bone, adipose tissue and mammary gland, among others (Pohjanvirta and Nasri, 2022). In vivo and in vitro studies show that 8PN has a beneficial effect on osteogenesis, prevents bone loss and improves biomechanical bone properties (Hümpel *et al.*, 2005; Sehmisch *et al.*, 2008; Ming *et al.*, 2013; Luo *et al.*, 2014).

Since phytoestrogens act via ER, there is a justified concern that they, especially the more potent ones (such as 8PN), might have adverse effects on estrogen-sensitive organs, such as uterus, vagina, and mammary gland (Rimoldi *et al.*, 2006; Štulíková *et al.*, 2018). Different trophic effects of 8PN on reproductive organs have been described, from negligible to significant, depending on the dose and study design, and information about estrogenic effects on the reproductive organs could be important for the assessment of safety of putative 8PN therapy in humans. (Hümpel *et al.*, 2005; Christoffel *et al.*, 2006; Rimoldi *et al.*, 2006; Keiler *et al.*, 2015; Štulíková *et al.*, 2018).

To date, there is no data about the effect of bisphosphonate and hop extract combination therapy on the osteoporosis and reproductive organs. In this paper we investigated the effect of alendronate, hop extract and their combination on uterine morphology of ovariectomized Wistar rats. We hereby also demonstrate a method for measuring rat uterus morphology, which can easily be adapted to suit the analysis of whole-slide images of almost any hollow organ, such as cross-sections of blood vessels or intestines. Results of these analyses are supplemented by manually assessed Ki67 expression.

MATERIAL AND METHODS

ANIMALS AND STUDY DESIGN

The study was approved by ethical committees of Faculty of Science, University of Zagreb (Approval Code: 251-58-10617-19-704) and Faculty of Medicine Osijek (Approval Code: 2158-61-46-22-16), as well as Croatian National ethical committee for protection of laboratory animals (EP 233/2020). Care and handling of the animals were in line with current international ethical norms, such as the Croatian law (Law on the Welfare of Animals, NN135/06 and NN37/13), EU Directive 2010/63/EU for animal experiments and Guide for the Care and Use of Laboratory Animals (National Research Council (US) Committee for the Update of the Guide for the Care and Use of Laboratory Animals., 2011).

A total of 68 six month old female Wistar rats were divided into 7 groups, 9 - 10 rats per group. Six groups were ovariectomized, while the control group underwent a sham operation. The 6 ovariectomized groups were: 1) untreated (OV, receiving 1 mL of intragastric (IG) propylene glycol, vehicle for the hop extract), 2) alendronate-low (AL, receiving 1 mg/kg IG alendronate), 3) alendronate-high (AH, receiving 2 mg/kg IG alendronate), 4) alendronate-low + hop extract (AL-X, receiving 1 mg/kg IG alendronate and 60 mg/kg hop extract), 5) alendronate-high + hop extract (AH-X, receiving 2 mg/kg IG alendronate and 60 mg/kg hop extract), and 6) hop extract (X, receiving 60 mg/kg hop extract). The control group also received 1 mL of IG propylene glycol. The animals were anesthetized using sevoflurane, sacrificed and uteri were fixed in 4 % paraformaldehyde. Middle third part of each uterus was embedded into paraffin blocks, and cut on a rotary microtome (Slee CUT 4060, Slee, Mainz, Germany) into 6 µm slides.

Alendronate was used as Alendox 70 (Belupo, Koprivnica, Croatia), for hop extract XanthoFlav was used (Hopsteiner, New York, USA), and sevoflurane was used as Sevorane (Abbott Laboratories, Chicago, Illinois, USA). According to HPLC analysis, XanthoFlav extract contained 75% xanthohumol, 0,4% isoxanthohumol, 0,3% 8-prenylnaringenin and 1,7% 6-prenylnaringenin.

UTERINE MORPHOLOGY

Slides stained with hematoxylin and eosin were photographed using Axiovert 200M microscope and Axiocam MRc camera (Carl Zeiss, Oberkochen, Germany). The whole slide was scanned under a 20 × objective as separate tiles forming a grid. The tiles were stitched together using Grid/Collection stitching plugin in FIJI distribution (Schindelin *et al.*, 2012), and an image of the whole uterus cross-section was obtained for each slide. Stitched images were manually processed in GIMP software to obtain color masks of endometrial layer, lumen, and total uterine tissue (Fig.1).

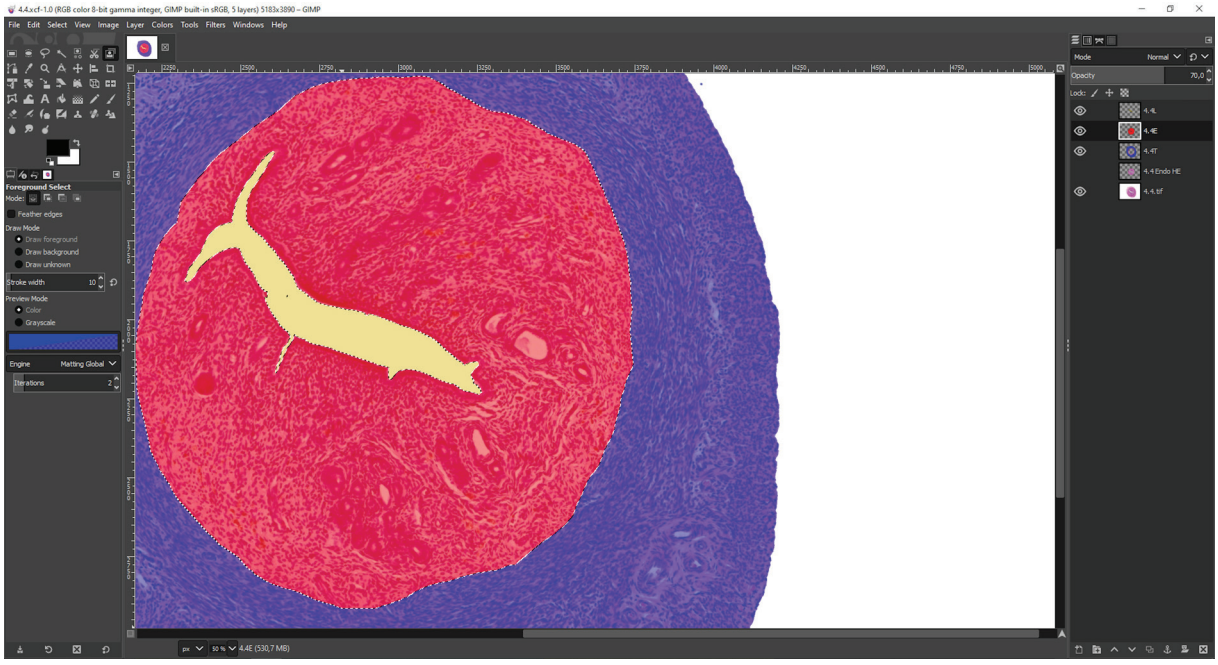

Fig. 1. *Creating color masks in Gimp. Image shows editable semi-transparent masks representing each layer of the uterus (myometrium and perimetrium in blue, endometrium in red and lumen in yellow), each mask on a separate layer of the image.*

The endometrium area and total uterus cross-section area were measured using FIJI. Share of endometrium area in total uterus area was calculated. The average thickness of the endometrium and whole uterus was measuredusing a custom-written macro in FIJI (see supplementary material). The ratio of average endometrium thickness and average total uterus thickness was calculated. First input for the macro were the previously made color masks of the lumen that were used to find the center of mass. Center of mass coordinates were then used to perform polar transformation on mask images of the endometrium or whole uterus cross-section using the Polar transformer plugin for FIJI (Available at: https://imagej.nih.gov/ij/plugins/polar-transformer.html). Polar transformer "unfolds" the masks taking a line for each of 360° viewed from the center of mass coordinates of a round object and creates a linear output image (Fig. 2). Using the macro, each row of pixels (representing 1°) was analyzed for white or black pixels using the histogram function. The sum of black pixels in each row was stored in a comma-separated value (.csv) file and the average value of the 360 measurements was used as the average thickness. Based on the pixel to micrometer ratio, pixel values were converted to micrometers. Share of the endometrium area or average thickness in whole uterus area or average thickness were statistically analyzed in Past software (Ham-mer *et al.*, 2001) using ANOVA with Tukey-Kramer *post hoc* test.

KI67 EXPRESSION

Ki67 immunohistochemical (IHC) staining was performed on an automatic VENTANA BenchMark Ultra IHC stainer (Roche, Basel, Switzerland). Rabbit monoclonal anti-Ki67 primary antibody produced by Roche (REF 791-4286) was used as recommended by supplier. Signal visualization was performed using UltraView Universal DAB Detection kit by Roche (REF 760-500). Slides were counterstained with hematoxylin as part of IHC stainer's protocol, manually dehydrated and coverslipped using automatic coverslipper Dako Sakura (Agilent, California, USA). Reaction buffer (Roche, REF 950-300) without primary antibody was used as negative control. The nuclear staining for Ki67 was assessed manually by an expert pathologist, using the AXIO Imager Microscope (Zeiss, Oberkochen, Germany). The tissues included in the analysis were: luminal epithelium (LE), glandular epithelium (GE), endometrial stroma (S) and myometrium (M). Strong nuclear Ki67 signal was counted in five consecutive high-power fields (40 × objective), which provides around 500 cells for analysis (Kinra and Malik, 2020). Results were analyzed using Kruskal-Wallis test with Dunn's post hoc and Bonferroni's correction in Past software (Hammer *et al.*, 2001).

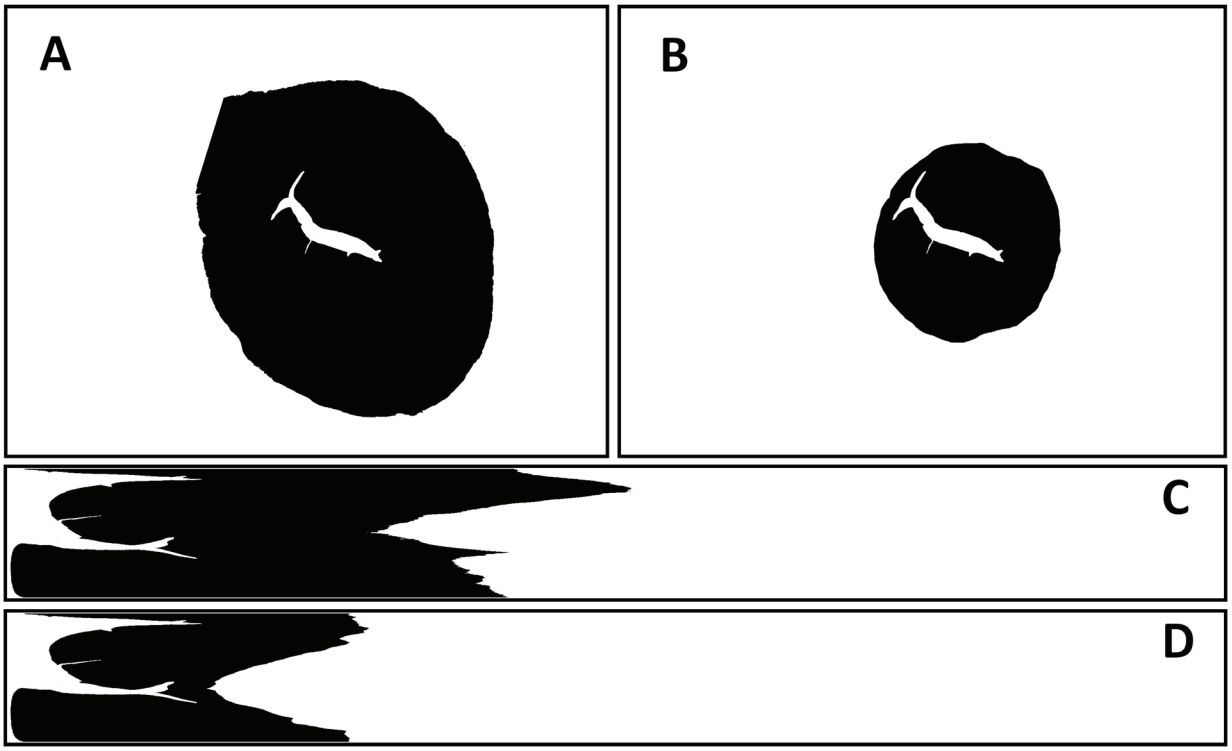

Fig. 2. *Polar transformation of the prepared masks. Original mask of whole uterus cross-section (A); original mask of endometrium cross-section (B); polar transformation of image A (C); polar transformation of image B (D).*

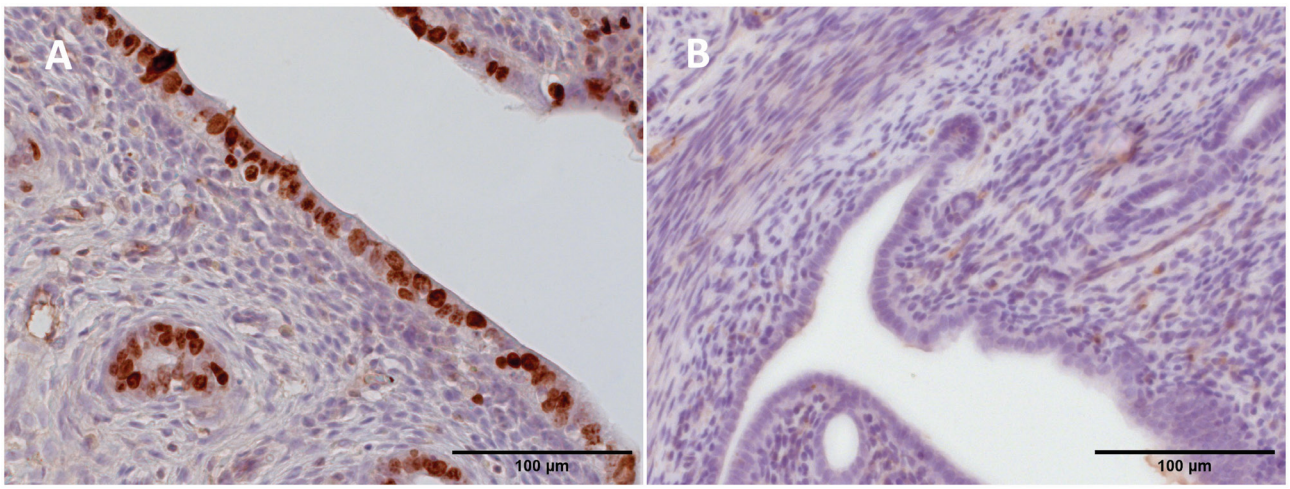

Fig. 3. *Ki67 expression. Image is showing part of the endometrium stained for Ki67 (A) and a negative control (B). Ki67 signal is visible in the nuclei of the lining and glandular epithelium, as well as several stromal cells. Objective 40 ×, scale bar 100 µm.*

RESULTS

UTERINE MORPHOLOGY

Brightfield microscopy examination revealed normal uterine morphology. As expected, the sham control group had significantly larger organs with endometrium morphology corresponding to normal estrous cycle. The ovariectomized groups had noticeably thinner endometrium, with markedly less glands and connective tissue (Fig. 4).

Once the masks were created and loaded in FIJI, our custom macro transformed the masks to linear images and measured the average thickness successfully. The share of endometrium area in total uterine cross-section area and the share of endometrium thickness in total uterine thickness were significantly higher in the control group than in all the ovariectomized groups. As for the ovariectomized groups, no significant differences were found in the measured values. Regardless of the treatment, the endometrium measurements were similar to the OV group (Fig. 4).

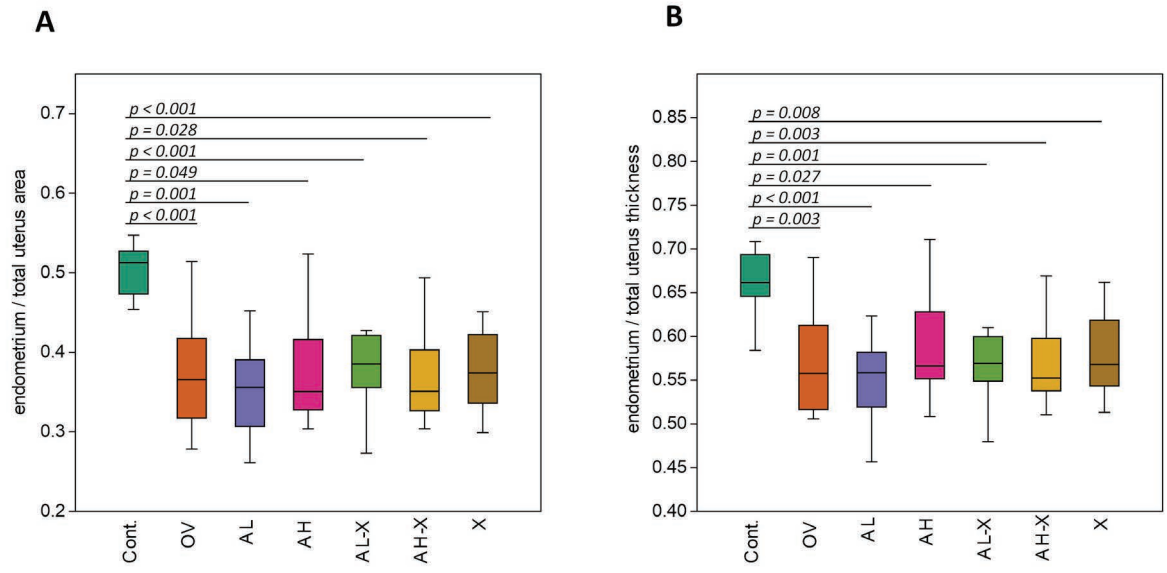

Fig. 4. *Results of morphometric analysis. Ratio of endometrium area in total uterine area (A); ratio of endometrium thickness in total uterine thickness (B). Cont. – control group; OV – ovariectomized untreated group; AL – low dose alendronate; AH – high dose alendronate; AL-X – alendronate-low and hop extract; AH-X – alendronate-high and hop extract; X – hop extract. Significant p values are shown on the graphs.*

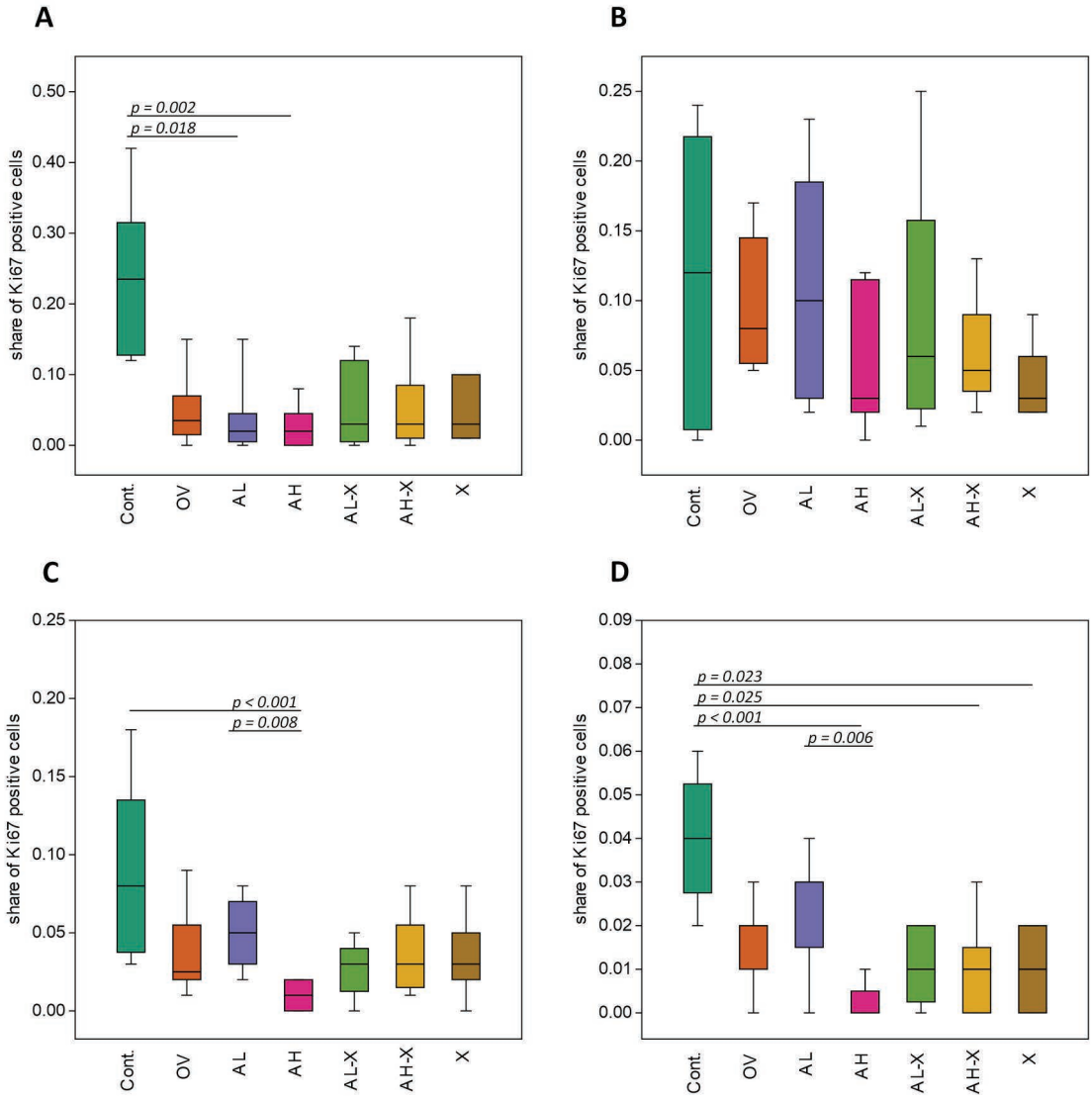

Fig. 5. *Analysis of Ki67 expression. Share of Ki67 positive cells in luminal epithelium (A), glandular epithelium (B), stroma (C) and myometrium (D). Cont. – control group; OV – ovariectomized untreated group; AL – low dose alendronate; AH – high dose alendronate; AL-X – alendronate-low and hop extract; AH-X – alendronate-high and hop extract; X – hop extract. Significant p values are shown on the graphs.*

KI67 EXPRESSION

Under a brightfield microscope, clear Ki67 IHC staining was observed on all slides (Fig. 3). Some false positives detected in small blood vessels were ignored during the analysis. In all the investigated tissues (LE, GE, S and M), the highest level of Ki67 expression was found in the control group, although not all of it was statistically significant (Fig. 5). Ki67 expression in the LE was significantly lower in groups treated with alendronate (both high and low dose), than in the sham-operated group. In the GE, no significant changes in Ki67 expression were found. In the S, significantly lower Ki67 expression was found in the AH group, compared to both control group and AL group. As for the M, Ki67 expression was significantly lower in AH, AH-X and X group than in the control group, and it should be noted that AL-X group was near borderline significance ($p = 0.078$). In the M, Ki67 expression was also significantly lower in the AH group compared to the AL group.

DISCUSSION

The significantly larger thickness and area of the endometrium in the control group was expected, as these

animals had ovaries and normal exposure to sex hormones. Nevertheless, the fact that other groups did not differ significantly shows that neither the hop extract, alendronate, nor their combination caused any significant proliferation of the endometrium. In the light of some concerns about phytoestrogen therapy for osteoporosis due to its potentially proliferative effects, our results suggest that hop extract, alone or in combination with alendronate, may be safe for use regarding the proliferative effects on endometrium in the given dose range. In fact, endometrial cancer risk is already known to be decreased by alendronate therapy for osteoporosis (Newcomb *et al.*, 2015). Therefore, our results suggest that alendronate and hop extract combination should be safe in this regard.

Ki67 is a marker of cellular proliferation, often used to assess the proliferative activity of malignant tumors. It is considered a clinically relevant marker in endometrial cancer (Kitson *et al.*, 2017). Reduction of Ki67 expression in ovariectomized groups was expected, since the sex hormones are directly involved in regulation of cellular proliferation in the uterine tissues (Quarmby and Korach, 1984; Marusak *et al.*, 2007). Furthermore, in some tissues, a significant or near-significant decrease in Ki67 expression was seen in alendronate-treated groups, especially in the AH group. This is consistent with other research which shows that bisphosphonate therapy lowers Ki67 in different tissues (Soydan *et al.*, 2015; Kassab, 2019; Sung *et al.*, 2020). The association of bisphosphonate therapy with a reduced risk of postmenopausal endometrial cancer seems logical in the context of lower expression of Ki67, an indicator of cellular proliferation, however, the mechanisms behind this phenomenon are still unclear (Newcomb *et al.*, 2015). This effect of bisphosphonate therapy may alleviate concerns regarding the possible proliferative effect of phytoestrogen therapy if used concomitantly with bisphosphonates. In our study, hop extract did not have a proliferative effect similar to estrogen. According to recent research, phytoestrogens can have different effects on female genital tract, but this varies with different phytoestrogens and one of the effects is reduced risk of endometrial cancer in humans (Burton and Wells, 2002). Therefore, our research suggests that alendronate and hop extract, alone or in combination therapy, do not cause proliferation of uterine tissues, and can even have a certain antiproliferative effect. It should be noted that, due to already mentioned biotransformation of xanthohumol into 8PN, most of the hop extract effects could be via 8PN.

It was interesting to see that Ki67 expression was significantly higher in the AL group than in the AH group in myometrium, and stroma. This might suggest that the effect of alendronate on the proliferation of cells in the myometrium is dose-dependent. Nevertheless, this was not present between AL-X and AH-X groups. Therefore, the effect of alendronate and hop extract may be additive in this respect. However, the difference between these groups and OV group was not significant, so the actual importance of these results is unclear. Further investigation of this effect is needed.

In the past, we have successfully used free and open-source software for research projects, e.g. for measurements of trabecular bone, aortae and femoral arteries (Bijelić *et al.*, 2017, 2022; Kozina *et al.*, 2019). The method we used to measure uterine morphology was developed as we were looking for a method more precise and unbiased for measurement of hollow organs than some older methods (such as drawing a target over the organ and measuring several diameters or measuring the longest and shortest radius/diameter). In our method we made 360 measurements, one for each degree from the center of mass. An average of 360 measurements gives a more precise result than just several measurements since many hollow organs are of irregular shape and morphology of their layers can vary on the cross-section. Our method can be easily adapted for measurement of any relatively round organ cross-section.

The method itself is semi-automated as multi-layered organs, such as uterus and blood vessels, have to be segmented first in order to identify the layers of interest (such as endometrium or myometrium). This needs to be done by an experienced histologist or pathologist. Although selection and segmentation can be done in FIJI, manual segmentation in Gimp has many advantages, e.g. selecting in multiple layers, using transparency function, easy editing of the selection, much more extensive undo/redo functions etc. This allows for meticulous annotation and preparing of masks that can be easily measured in FIJI using our macro. Another advantage of using Gimp is saving of the .xcf files with all the layers and selections intact for later review and modification as needed.

We have considered several programs for counting Ki67, however, in this paper, we decided to assess it manually by a pathologist. Although there are fine programs and plugins for measuring IHC signal, such software may not always be 100% accurate, which depends not only on the software itself, but also on the strength of IHC staining, possible background staining, false positives, and the counterstain. The common errors that come from usage of automated analysis include fragmenting one positive nucleus into 2 or more, merging of several positive nuclei, failing to detect weakly stained nuclei, identifying cytoplasmic staining and endothelial cells etc. Manual preparation and editing of these images

to achieve good results with automated counting would be too time consuming in our case. On the other hand, some groups have reported good results, some of them with free and open-source software, such as QuPath and ImageJ (Feng *et al.*, 2020; Boyaci *et al.*, 2021), but there is still room for improvement, both in free and commercial software (Vesterinen *et al.*, 2022). This is an active field of research and, hopefully, the results may allow for full automatization of the positive cell counting in the future.

In conclusion, our semi-automated method enables precise and unbiased analysis of whole-slide images of almost any round or oval organ using free and open-source software. To our knowledge, this is the first paper dealing with the impact of combination therapy with alendronate and hop extract on uterine morphology in osteoporosis model.

ACKNOWLEDGMENT

The hop extract XanthoFlav was generously donated by Hopsteiner company. The authors wish to thank Ms Danica Matić for her invaluable help in the histology lab.

REFERENCES

Aeffner F, Zarella MD, Buchbinder N, Bui MM, Goodman MR, Hartman DJ, Lujan GM, Molani MA, Parwani A V., Lillard K, Turner OC, Vemuri VNP, Yuil-Valdes AG, Bowman D (2019). Introduction to Digital Image Analysis in Whole-slide Imaging: A White Paper from the Digital Pathology Association. J Pathol Inform 10:9. https://doi.org/10.4103/jpi.jpi_82_18

An K-C (2016). Selective Estrogen Receptor Modulators. Asian Spine J 10:787–91. https://doi.org/10.4184/asj.2016.10.4.787

Bijelić N, Belovari T, Stolnik D, Lovrić I, Baus Lončar M (2017). Histomorphometric Parameters of the Growth Plate and Trabecular Bone in Wild-Type and Trefoil Factor Family 3 (Tff3)-Deficient Mice Analyzed by Free and Open-Source Image Processing Software. Microsc Microanal 23:818–25. https://doi.org/10.1017/S1431927617000630

Bijelić N, Kozina N, Rođak E, Iva B, Šešelja K, Baus Lončar M, Belovari T, Jukić I, Drenjančević I, Bazina I, Šešelja K, Baus Lončar M, Belovari T, Jukić I, Drenjančević I (2022). Structural characteristics of femoral arteries in wild-type and TFF3 knock-out mice on standard and high-salt diet. In 4th Croatian Microscopy Congress with international participation (eds. J. Macan, G. Kovačević), pp. 34–5. Poreč, Hrvatska.

Boyaci C, Sun W, Robertson S, Acs B, Hartman J (2021). Independent Clinical Validation of the Automated Ki67 Scoring Guideline from the International Ki67 in Breast Cancer Working Group. Biomolecules 11:1612. https://doi.org/10.3390/biom11111612

Burel JM, Besson S, Blackburn C, Carroll M, Ferguson RK, Flynn H, Gillen K, Leigh R, Li S, Lindner D, Linkert M, Moore WJ, Ramalingam B, Rozbicki E, Tarkowska A, Walczysko P, Allan C, Moore J, Swedlow JR (2015). Publishing and sharing multi-dimensional image data with OMERO. Mamm Genome 26:441–7. https://doi.org/10.1007/S00335-015-9587-6/FIGURES/1

Burton JL, Wells M (2002). The effect of phytoestrogens on the female genital tract. J Clin Pathol 55:401–7. https://doi.org/10.1136/jcp.55.6.401

Chen M-N, Lin C-C, Liu C-F (2015). Efficacy of phytoestrogens for menopausal symptoms: a meta-analysis and systematic review. Climacteric 18:260–9. https://doi.org/10.3109/13697137.2014.966241

Christoffel J, Rimoldi G, Wuttke W (2006). Effects of 8-prenylnaringenin on the hypothalamo-pituitary-uterine axis in rats after 3-month treatment. J Endocrinol 188:397–405. https://doi.org/10.1677/joe.1.06384

Dobbs MB, Buckwalter J, Saltzman C (1999). Osteoporosis: the increasing role of the orthopaedist. Iowa Orthop J 19:43–52.

Drake MT, Clarke BL, Khosla S (2008). Bisphosphonates: mechanism of action and role in clinical practice. Mayo Clin Proc 83:1032–45. https://doi.org/10.4065/83.9.1032

Ensrud KE, Crandall CJ (2017). Osteoporosis. Ann Intern Med 167:17–32. https://doi.org/10.7326/AITC201708010

Feng M, Deng Y, Yang L, Jing Q, Zhang Z, Xu L, Wei X, Zhou Y, Wu D, Xiang F, Wang Y, Bao J, Bu H (2020). Automated quantitative analysis of Ki-67 staining and HE images recognition and registration based on whole tissue sections in breast carcinoma. Diagn Pathol 15:65. https://doi.org/10.1186/s13000-020-00957-5

Fu S, Zeng G, Zong S, Zhang Z, Zou B, Fang Y, Lu L, Xiao D (2014). Systematic review and meta-analysis of the bone protective effect of phytoestrogens on osteoporosis in ovariectomized rats. Nutr Res 34:467–77. https://doi.org/10.1016/j.nutres.2014.05.003.

Guo J, Nikolic D, Chadwick LR, Pauli GF, van Breemen RB (2006). Identification of human hepatic cytochrome P450 enzymes involved in the metabolism of 8-prenylnaringenin and isoxanthohumol from hops (Humulus lupulus L.). Drug Metab Dispos 34:1152–9. https://doi.org/10.1124/dmd.105.008250

Hammer DAT, Ryan PD, Hammer Ø, Harper DAT (2001). Past: Paleontological Statistics Software Package for Education and Data Analysis. Palaeontol Electron 4:178.

Hümpel M, Isaksson P, Schaefer O, Kaufmann U, Ciana P, Maggi A, Schleuning W-D (2005). Tissue specificity of 8-prenylnaringenin: protection from ovariectomy induced bone loss with minimal trophic effects on the uterus. J Steroid Biochem Mol Biol 97:299–305. https://doi.org/10.1016/j.jsbmb.2005.05.009

Ji M-X, Yu Q (2015). Primary osteoporosis in postmenopausal women. Chronic Dis Transl Med 1:9–13. https://doi.org/10.1016/j.cdtm.2015.02.006

Kassab A (2019). Effect of Fosamax on the duodenal mucosa in adult male albino rats and the possible protection by nigella sativa oil: a histological and immunohistochemical study. Egypt J Histol 42: 900-14. https://doi.org/10.21608/ejh.2019.10902.1105

Keiler AM, Dörfelt P, Chatterjee N, Helle J, Bader MI, Vollmer G, Kretzschmar G, Kuhlee F, Thieme D, Zierau O (2015). Assessment of the effects of naringenin-type flavanones in uterus and vagina. J Steroid Biochem Mol Biol 145:49–57. https://doi.org/10.1016/j.jsbmb.2014.10.00

Kinra P, Malik A (2020). Ki 67: Are we counting it right? Indian J Pathol Microbiol 63:98–99. https://doi.org/10.4103/IJPM.IJPM_770_19

Kitson S, Sivalingam VN, Bolton J, McVey R, Nickkho-Amiry M, Powell ME, Leary A, Nijman HW, Nout RA, Bosse T, Renehan AG, Kitchener HC, Edmondson RJ, Crosbie EJ (2017). Ki-67 in endometrial cancer: scoring optimization and prognostic relevance for window studies. Mod Pathol 30:459–68 https://doi.org/10.1038/modpathol.2016.203

Kozina N, Mihaljević Z, Baus Lončar M, Mihalj M, Mišir M, Radmilović M, Justić H, Gajović S, Šešelja K, Bazina I, Horvatić A, Matić A, Bijelić N, Rođak E, Jukić I, Drenjančević I (2019). Impact of High Salt Diet on Cerebral Vascular Function and Stroke in Tff3−/−/C57BL/6N Knockout and WT (C57BL/6N) Control Mice. Int J Mol Sci 20:5188. https://doi.org/10.3390/ijms20205188

Luo D, Kang L, Ma Y, Chen H, Kuang H, Huang Q, He M, Peng W (2014). Effects and mechanisms of 8-prenylnaringenin on osteoblast MC3T3-E1 and osteoclast-like cells RAW264.7. Food Sci Nutr 2:341–50. https://doi.org/10.1002/fsn3.109

Marusak RA, Radi ZA, Obert L (2007). Expression of Ki-67 in the uterus during various stages of the estrous cycle in rats. Exp Toxicol Pathol 59:151–55. https://doi.org/10.1016/j.etp.2007.06.004

Ming L-G, Lv X, Ma X-N, Ge B-F, Zhen P, Song P, Zhou J, Ma H-P, Xian CJ, Chen K-M (2013). The prenyl group contributes to activities of phytoestrogen 8-prenynaringenin in enhancing bone formation and inhibiting bone resorption in vitro. Endocrinology 154:1202–14. https://doi.org/10.1210/en.2012-2086

National Research Council (US) Committee for the Update of the Guide for the Care and Use of Laboratory Animals. (2011). Guide for the Care and Use of Laboratory Animals. National Academies Press, Washington, D.C.

Newcomb PA, Passarelli MN, Phipps AI, Anderson GL, Wactawski-Wende J, Ho GYF, O'Sullivan MJ, Chlebowski RT (2015). Oral bisphosphonate use and risk of postmenopausal endometrial cancer. J Clin Oncol 33:1186–90. https://doi.org/10.1200/JCO.2014.58.6842

Pohjanvirta R, Nasri A (2022). The Potent Phytoestrogen 8-Prenylnaringenin: A Friend or a Foe? Int J Mol Sci 23:3168. https://doi.org/10.3390/ijms23063168

Possemiers S, Bolca S, Grootaert C, Heyerick A, Decroos K, Dhooge W, De Keukeleire D, Rabot S, Verstraete W, Van de Wiele T (2006). The Prenylflavonoid Isoxanthohumol from Hops (Humulus lupulus L.) Is Activated into the Potent Phytoestrogen 8-Prenylnaringenin In Vitro and in the Human Intestine. J Nutr 136:1862–67. https://doi.org/10.1093/jn/136.7.1862

Quarmby VE, Korach KS (1984). The influence of 17 beta-estradiol on patterns of cell division in the uterus. Endocrinology 114:694–702. https://doi.org/10.1210/endo-114-3-694

Rimoldi G, Christoffel J, Wuttke W (2006). Morphologic changes induced by oral long-term treatment with 8-prenylnaringenin in the uterus, vagina, and mammary gland of castrated rats. Menopause 13:669–77. https://doi.org/10.1097/01.gme.0000196596.90076.d0

Rueden CT, Schindelin J, Hiner MC, DeZonia BE, Walter AE, Arena ET, Eliceiri KW (2017). ImageJ2: ImageJ for the next generation of scientific image data. BMC Bioinformatics 18:1–26. https://doi.org/10.1186/S12859-017-1934-Z/FIGURES/7

Schindelin J, Arganda-Carreras I, Frise E, Kaynig V, Longair M, Pietzsch T, Preibisch S, Rueden C, Saalfeld S, Schmid B, Tinevez J-Y, White DJ, Hartenstein V, Eliceiri K, Tomancak P, Cardona A (2012). Fiji: an open-source platform for biological-image analysis. Nat Methods 9:676–82 https://doi.org/10.1038/nmeth.2019

Schneider CA, Rasband WS, Eliceiri KW (2012). NIH Image to ImageJ: 25 years of image analysis. Nat Methods 9:671–75 https://doi.org/10.1038/nmeth.2089

Sedgewick J (2017). Acquisition and Post-Processing of Immunohistochemical Images. In Methods in molecular biology (Clifton, N.J.), pp. 75–106. Methods Mol Biol.

Sehmisch S, Hammer F, Christoffel J, Seidlova-Wuttke D, Tezval M, Wuttke W, Stuermer KM, Stuermer EK (2008). Comparison of the phytohormones genistein, resveratrol and 8-prenylnaringenin as agents for preventing osteoporosis. Planta Med 74:794–801. https://doi.org/10.1055/s-2008-1074550

Słupski W, Jawień P, Nowak B (2021). Botanicals in Postmenopausal Osteoporosis. Nutrients 13:1609. https://doi.org/10.3390/nu13051609

Solomon RW (2009). Free and Open Source Software for the Manipulation of Digital Images. Am J Roentgenol 192:W330–34. https://doi.org/10.2214/AJR.08.2190

Soydan SS, Araz K, Senel F V., Yurtcu E, Helvacioglu F, Dagdeviren A, Tekindal MA, Sahin F (2015). Effects of alendronate and pamidronate on apoptosis and cell proliferation in cultured primary human gingival fibroblasts. Hum Exp Toxicol 34:1073–82. https://doi.org/10.1177/0960327115569808

Štulíková K, Karabín M, Nešpor J, Dostálek P (2018). Therapeutic Perspectives of 8-Prenylnaringenin, a Potent Phytoestrogen from Hops. Molecules 23:660. https://doi.org/10.3390/molecules23030660

Sung C-M, Kim RJ, Hah Y-S, Gwark J-Y, Park H Bin (2020). In vitro effects of alendronate on fibroblasts of the human rotator cuff tendon. BMC Musculoskelet Disord 21:19. https://doi.org/10.1186/s12891-019-3014-1

Tella SH, Gallagher JC (2014). Prevention and treatment of postmenopausal osteoporosis. J Steroid Biochem Mol Biol 142:155–70. https://doi.org/10.1016/j.jsbmb.2013.09.008

Vesterinen T, Säilä J, Blom S, Pennanen M, Leijon H, Arola J (2022). Automated assessment of Ki-67 proliferation index in neuroendocrine tumors by deep learning. APMIS 130:11–20 https://doi.org/10.1111/apm.13190